Isomeric gamma rays from $^{235}U(n,f)$ and $^{239}Pu(n,f)$ for times less than 1 μsec after fission*

R. E. Sund,† Hans Weber, and V. V. Verbinski
Intelcom Rad Tech, San Diego, California 92138
(Received 20 May 1974)

Measurements of the isomeric γ-ray energy spectra from the thermal-neutron fission of ^{235}U and ^{239}Pu were performed with a Ge(Li) detector for times between 20 nsec and $\sim$1 μsec after fission. Eighty resolved γ-ray peaks with different energies and half-lives were observed; 37 of these γ-ray peaks had not been seen in previous delayed γ-ray measurements. The fission-fragment mass numbers for many of the γ rays were determined by comparison of the γ-ray energies and half-lives with the results of previous ^{252}Cf measurements. γ rays which decay in cascade from the same isomeric state were identified on the basis of mass numbers, γ-ray half-lives, and intensities. Isomeric γ-ray spectra from the spontaneous fission of ^{252}Cf were also measured in the present experiment; the analysis of a number of strong, resolved γ rays in these data indicated that the present results are consistent with previous ^{252}Cf results, within the sum of the systematic uncertainties of the two experiments. The total energy of the resolved peaks from this experiment, when integrated over all time, is 163 and 164 keV/fission for ^{235}U and ^{239}Pu, respectively. Roughly 40% of the total energy of the resolved peaks is from γ rays in the 1100- to 1340-keV region. Isomers in $^{134}_{52}Te_{82}$ and $^{136}_{54}Xe_{82}$ contribute most of these high-energy γ rays. In the 140- to 1340-keV energy range and 20- to 958-nsec time interval, the energy of the observed continuum of unresolved γ rays was $\sim$20 and $\sim$24% of the total delayed γ-ray energy for ^{235}U and ^{239}Pu, respectively. The energy of the resolved γ rays from this experiment for ^{235}U and ^{239}Pu is about twice that for the isomers from ^{252}Cf with the same range of half-lives, as observed from previous results. Most of the difference between ^{252}Cf and ^{235}U or ^{239}Pu is due to seven possible γ-ray cascades.

[NUCLEAR REACTIONS, FISSION $^{235}U(n,f)$, $^{239}Pu(n,f)$, and ^{252}Cf, measured isomeric γ-ray E_γ, $T_{1/2}$; 20–1000 nsec; measured E_γ (total), deduced A; Ge(Li) with unfolding; 85–4000 keV.]

1. INTRODUCTION

The number, energy, and half-life of the isomeric γ rays emitted per neutron fission of ^{235}U and ^{239}Pu were measured for times between 20 nsec and ~1 μsec after fission. In this time region no previous delayed γ-ray measurements have been reported for ^{239}Pu, and a few measurements have been performed for ^{235}U with only limited results. Delayed γ rays in this time region were first observed by Maienschein *et al.* (Ref. 1) in measurements between 50 nsec and 1.4 μsec after $^{235}U(n,f)$; their pulse-height data, which were taken with a small NaI detector and which were not unfolded to obtain energy spectra, showed three prominent γ-ray peaks with energies of 0.19, 0.30, and 1.3 MeV, and a decay with a half-life on the order of 100 nsec. A NaI detector was used by Popeko *et al.* (Ref. 2) to measure delayed γ rays from $^{235}U(n,f)$ in the time region from 10 to 70 nsec. They also presented unprocessed pulse-height data, and these results did not include events with pulse heights greater than 0.5 MeV.

In contrast to these early ^{235}U experiments, more detailed measurements of isomeric γ rays from ^{252}Cf spontaneous fission have been made. Measurements of delayed γ rays for times less than 300 nsec after the spontaneous fission of ^{252}Cf were made by Johansson (Ref. 3). NaI pulse-height distributions were obtained for various fission-fragment mass regions, as determined with the use of semiconductor counters. Time distributions of total γ-ray counts indicated half-lives in the 15- to 100-nsec region for three different broad ranges of fission-fragment mass ratios. In more recent measurements by John, Guy, and Wesolowski (Ref. 4) at Livermore, delayed γ rays emitted from 3 to 2000 nsec after the spontaneous fission of ^{252}Cf were studied to determine the energy, half-life, and intensity of each γ ray and the associated mass of the fission fragment. Two Si surface-barrier detectors were used to detect the fission fragments, and a Ge(Li) detector was used to measure the γ rays. The good resolution of the γ-ray detector overcame many of the limitations of previous isomeric γ-ray measurements for times less than 2 μsec after fission. In addition, the accurate determination of the mass of the fission fragment associated with each γ ray was a significant improvement over earlier measurements. The Livermore group reported a total of 144 γ rays in their results. Measurements of delayed γ rays from ^{252}Cf were also performed by Ajitanand, and a number of γ rays were observed in the 300-nsec to 5-μsec time region after fission (Ref. 5).

The present measurements are a continuation of a series of earlier efforts carried out at this

laboratory to measure the prompt and delayed γ rays from fission. The absolute yields of prompt γ rays from the thermal-neutron fission of ^{235}U and ^{239}Pu, and from the spontaneous fission of ^{252}Cf, were previously measured for times less than ~10 nsec after fission (Ref. 6). Prior to this, delayed γ rays in the time region from 2 μsec to ~0.1 sec after neutron fission, and from 2 μsec to 7 sec after photofission, were studied with the use of pulsed beams of bremsstrahlung and neutrons from an electron linear accelerator (Refs. 7–9). In the region between ~1 msec and 0.1 sec, the γ-ray intensities were found to decrease little; these γ rays mainly follow β decay (Refs. 7, 8). For times between 2 and 800 μsec, the γ-ray intensities decrease rapidly with increasing time; in this time region the γ rays from isomers produced in fission are the dominant source of delayed γ rays (Refs. 7–9). The present delayed γ-ray results essentially fill the gap which has existed in the ^{235}U and ^{239}Pu data from this and other laboratories for times between the prompt γ rays and the γ rays emitted later than 2 μsec after fission.

2. EXPERIMENTAL PROCEDURE

A TRIGA reactor, which operated at a power level of ~1 MW, served as the neutron source. A graphite thermal column, 0.9 m×0.9 m×1.5 m long, partly surrounded the reactor, providing a source of highly thermalized neutrons. Some of these neutrons passed down a 10-m-long, 0.15-m-diam hollow beam pipe to the fission foil. A 195-cm-long tapered neutron and γ-ray collimator was inserted into the beam pipe to allow an approximately end-on irradiation of the thin fissionable target by neutrons passing through the narrow, rectangular cross-section opening. Approximately 1 cm of lead was placed directly in the beam at 200 cm from the target to remove most of the low-energy γ rays. The neutron intensity at the target was ~10^6 neutrons/cm^2 sec.

The ^{235}U and ^{239}Pu were isotopically enriched to 99.44 and 99.98%, and deposited in the form of an oxide to a thickness of 1.0 and 0.7 mg/cm^2, respectively; the ^{252}Cf test source consisted of 0.02 μg of the isotope. Each of the three samples had a diameter of 2.5 cm. The ^{235}U and ^{252}Cf sources were deposited on a thin Be backing (with 0.0013-cm thickness) to reduce the production of neutron capture γ rays and to reduce the neutron and γ-ray scattering from the beam into the γ-ray detector. Because of Pu flaking problems on Be backings, the ^{239}Pu source for these measurements had a backing of 0.000 13-cm-thick Ni followed by 0.0013-cm-thick Be. The Be was added behind the nickel so that the attenuation of the fission fragments through the backing would be roughly the same for ^{235}U, ^{252}Cf, and ^{239}Pu. This was desirable, since the number of fission fragments which leave the back of the foil and stop on the backing holder, about 0.6 cm away, or stop on a 2.5-cm-diam cylindrical surface between the source and backing holder can affect the γ-ray detection efficiency. In the present case, this effect is small because most of the fragments are stopped in the Be backing.

The fission-fragment detectors were 950-mm^2 heavy-ion surface-barrier detectors. They were cooled to below −30°C, which greatly reduced the leakage current due to radiation damage from fission fragments and from α particles from ^{239}Pu and ^{252}Cf. Each detector frame was made of aluminum and protruded only ~0.1 cm from the detector surface. The detector was positioned ~0.2 cm from the fission sample so that most of the fission fragments could be detected. This reduced the chance coincidence background to an acceptable level, since a large fraction of the prompt γ rays were rejected on the basis of the time association with fission fragments. The remaining prompt γ rays were rejected with other chance backgrounds, as discussed below. The detector was located out of the direct neutron beam, where it would have produced a high background. The rate of radiation damage to a detector from ^{239}Pu α-particle irradiation was especially high; consequently, the total running time for each detector used with ^{239}Pu was limited to about 20 h. The fission-fragment detector and fission sample were held in a vacuum chamber designed to cool the detector, avoid fission-fragment energy loss in air, and minimize the scattering of the thermal-neutron beam into the γ-ray detector.

A true coaxial Ge(Li) detector with an active volume of 47 cm^3 was used as the γ-ray spectrometer. This detector had a peak-to-Compton ratio of ~28:1 and a resolution of ~2.3 keV at 1.33 MeV. The axis of the Ge(Li) detector was perpendicular to the neutron-beam direction, and this detector was located 5.3 cm from the fission sample.

To reduce the intensity of the low-energy γ rays from the natural radioactivity of ^{239}Pu to a reasonable level, a 0.011-cm-thick lead filter was placed between the fission foil and the Ge(Li) detector for all of the delayed γ-ray measurements, and also for measurements of detector efficiencies and responses with known γ-ray sources. In addition, a thin layer of ^{6}LiF was placed between the fissionable sample and γ-ray detector to stop the thermal neutrons scattered by the sample. The γ rays being measured also had to pass through the target vacuum-chamber window and the Ge(Li) detector cryostat, traversing a total

thickness of ~0.3-cm aluminum before reaching the Ge(Li) detector.

The Ge(Li) detector was calibrated by placing known γ-ray sources at the location of the fission target. The fission-fragment detector and a fission foil holder were left in their usual positions during the calibration, so that the backscatter-γ-ray contribution to the detector response was reproduced at each calibration energy. Measurements were taken as a function of the radial position of the sample to determine the variation of efficiency with radius. The results of the efficiency measurement are shown in Fig. 1. The sources and energies (in keV) of the γ rays used in the measurement are: ^{109}Cd, 88; ^{144}Ce, 133.6; ^{203}Hg, 279; ^{133}Ba, 303 and 356; ^{113}Sn, 393; ^{137}Cs, 662; ^{54}Mn, 835; ^{88}Y, 898 and 1836; ^{22}Na, 1275; ^{60}Co, 1173 and 1333; and ThC'', 2615. Calibrated ^{109}Cd, ^{137}Cs, ^{60}Co, and ThC'' sources were obtained from the National Bureau of Standards (NBS). The other sources were calibrated at this laboratory using a Ge(Li) γ-ray spectrometer system, which in turn had been calibrated with a series of NBS sources. The uncertainty in efficiency is ~±3%. The efficiency curve is drawn dotted below ~130 keV because of the higher uncertainty in this region where the 0.011-cm-thick lead filter mentioned above becomes important. The response functions were determined from measurements with the following sources and γ-ray energies in keV: ^{203}Hg, 279; ^{113}Sn, 393; ^{137}Cs, 662; ^{54}Mn, 835; ^{22}Na, 1275; ^{88}Y, 1836; and ThC'', 2615.

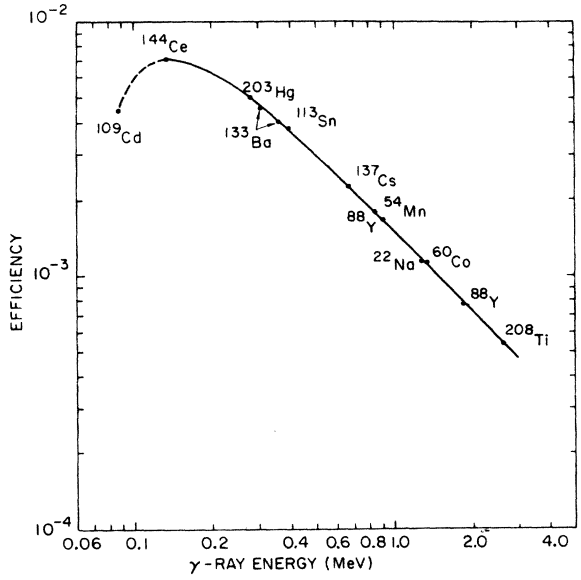

FIG. 1. Full-energy peak efficiency of Ge(Li) detector versus γ-ray energy, with the γ-ray sources located at the normal position of the fission foil and 0.011 cm of lead between source and detector.

The shape of the backscatter peak and the lower part of the Compton distribution for the 1275-keV γ ray from ^{22}Na was determined from the spectrum of the 1333- and 1173-keV γ rays from ^{60}Co. To determine the response function of the 1836-keV γ ray from ^{88}Y, the response function for the 898-keV γ ray from ^{88}Y was determined by interpolation from other sources and then subtracted from the total ^{88}Y data. Response functions for other energies were obtained by interpolation from the above measurements.

A schematic drawing of the electronic setup is shown in Fig. 2. The main functions of the electronics were to: (1) determine the time between γ-ray and fission-fragment events accurately through the use of fast timing; (2) determine the γ-ray energy accurately with the use of a stabilization system for gain and zero-energy channel; (3) sample the background for times preceding the fission event; (4) reject all events for which more than one γ-ray event occurred within the 25 μsec recovery time of the amplifier used with the γ-ray spectrometer; (5) reject all events, including background events, for which another fission event occurred for a period of about 2 μsec before and 1.2 μsec after the fission event under consideration; (6) provide the proper delays and coincidence-logic pulses necessary for correct data storage; and (7) count only the valid fission events, i.e., those that would have provided a valid count for either a delayed γ-ray or background event, with the restrictions of conditions (4) and (5) above.

The time at which the fission event occurred was determined within ~2 to 3 nsec by means of the fission-fragment detector, a fast preamplifier (Solid State Radiations-112), and a double-level, leading-edge discriminator. The lower-level discriminator provided the timing information for all pulses with amplitudes above the bias setting of the upper level. The bias of the lower level was set just above the amplitude of the noise and the α-particle pulses, and the bias of the upper level was set about 25% higher; this was well below the lower fission-fragment peak. The rise time of the fission-fragment pulse at the input of the leading-edge discriminator was about 10 nsec. The pulse decayed to the base line in ~25 nsec and then had a small overshoot which lasted 80 nsec. The number of fission-fragment pulses not rejected under criterion (5) above because of the overlap of pulses from the preamplifier was negligible at the count rates encountered in the experiment.

Because the delayed γ-rays were to be measured in the presence of very intense prompt γ rays, the timing of the γ-ray pulses had to be improved

beyond the state of the art for a large-volume Ge(Li) detector. The timing signal from the Ge(Li) detector was obtained by (a) demanding a triple coincidence between a leading-edge discriminator and two zero-crossing timing discriminators operated at two different time constants, and (b) adjusting the triple-coincidence time requirements so only the fast rise time pulses were accepted. The fraction of γ-ray pulses lost was carefully determined as a function of pulse height and remeasured at periodic intervals during the experiments by simply running an analyzer in the free mode, and then in the mode in which it was gated on by the output of the three-way coincidence circuit; the count-rate ratio at each energy gave the correction factor for the measured delayed γ-ray pulse-height distributions.

The timing of the circuitry was checked by substituting a plastic scintillator system with an Ortec fast, crossover timing base mounted on a phototube in place of the fission-fragment detector, and then measuring the γ-γ timing for the Ge(Li) and plastic scintillator system as a function of the energy for pulses from the Ge(Li) detector. The 1.33- and 1.17-MeV cascade γ rays from ^{60}Co were used in this fast timing measurement. The

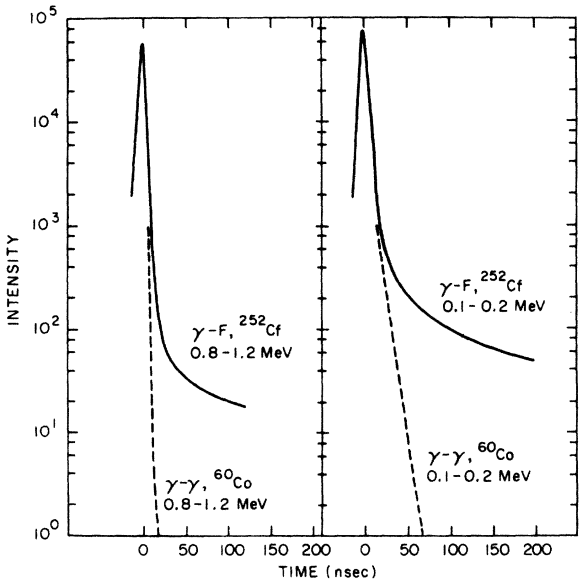

FIG. 3. Intensity of γ rays detected by the Ge(Li) detector as a function of time with respect to a fission event from ^{252}Cf (solid line) or with respect to a coincident γ-ray event from ^{60}Co (dashed line). The energy intervals of the analyzed pulse from the Ge(Li) detector are given on the figure.

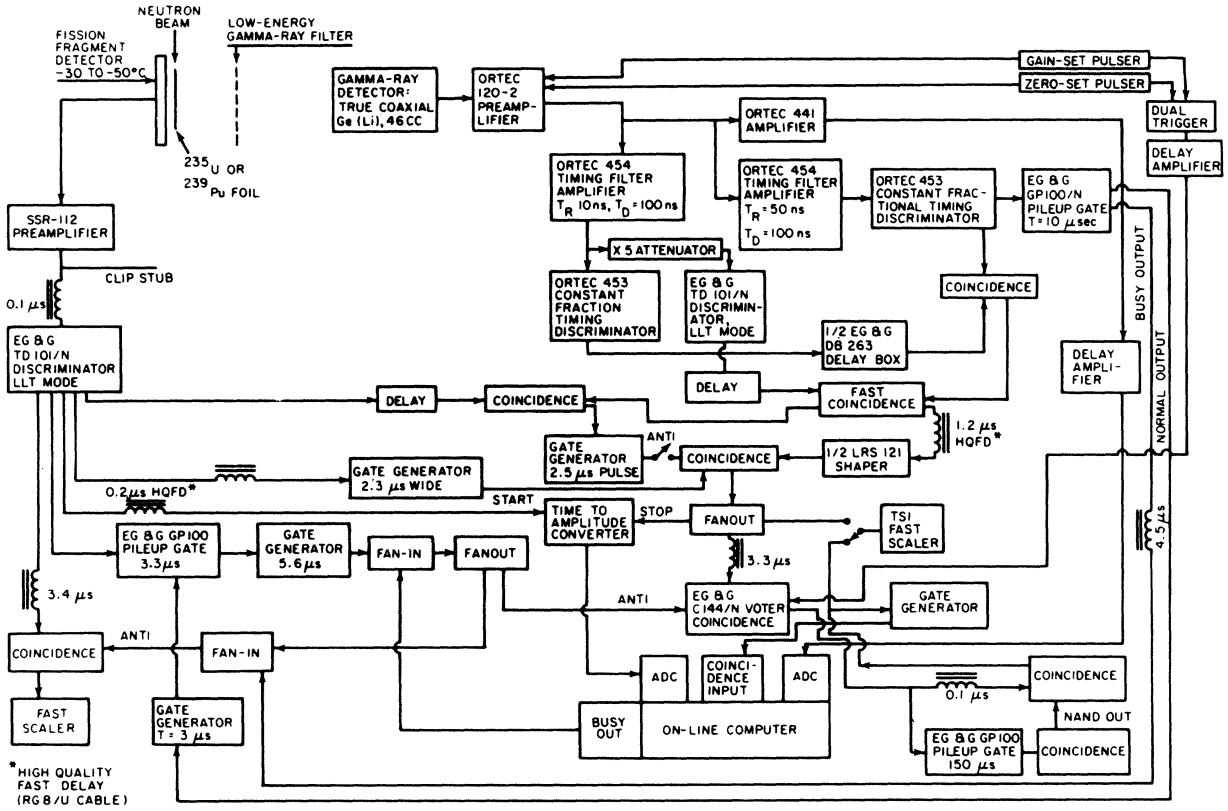

FIG. 2. Block diagram of electronics.

results are shown in Fig. 3 for events from the Ge(Li) detector that fall in the pulse-height ranges of 0.1 to 0.2 MeV and 0.8 to 1.2 MeV. Since timing for signals from both the plastic scintillator and the fission-fragment detector was very fast compared to that from the Ge(Li) detector, the γ-γ coincidence curves indicate the expected γ-ray timing uncertainties in the fission-fragment and Ge(Li) detector system. The 0.8- to 1.2-MeV and 0.1- to 0.2-MeV γ-γ time-slewing data show that the intensity is reduced by a factor of 10^3 in 10 and ~30 nsec, respectively. For comparison, the fission-fragment detector and Ge(Li) detector were used in coincidence to measure the time response for the prompt and delayed γ rays from the fission of ^{252}Cf; curves for the two detector systems were normalized at the peak for the data shown in Fig. 3. The 0.1- to 0.2-MeV data indicate that the ^{252}Cf delayed γ-ray signals at ~50 nsec are an order of magnitude higher than the prompt γ rays that are detected at ~50 nsec because of time slewing, and are much higher at later times. Also, the 0.8- to 1.2-MeV delayed γ-ray data at ~10 nsec are a factor of 10 higher than the time-slewed prompt γ rays detected at 10 nsec.

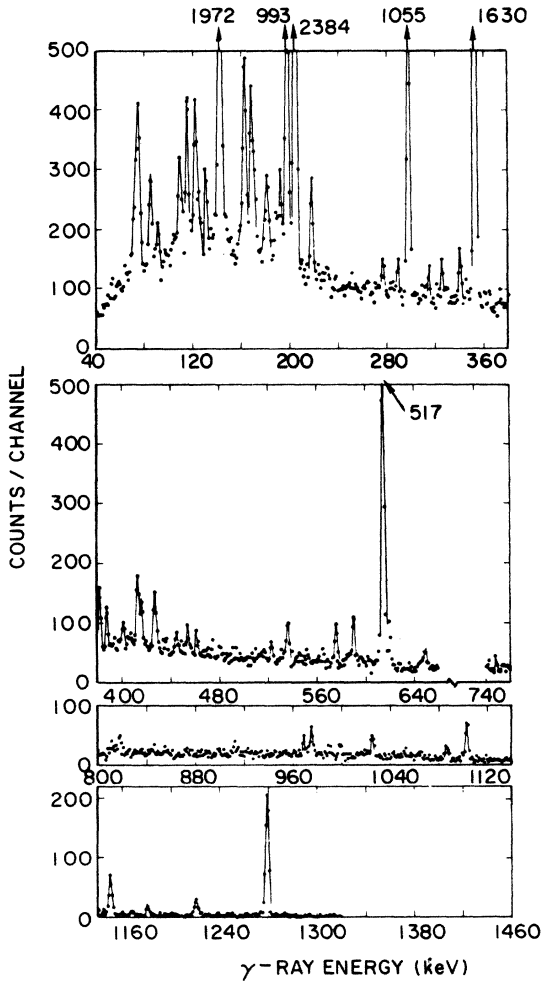

FIG. 4. Pulse-height distribution for γ rays emitted between 45 and 68 nsec after $^{235}U(n,f)$, uncorrected for the decrease in counts at low pulse heights due to the rejection of slow rise-time pulses.

The signals from the main electronic area at the detectors were sent to an on-line computer. The coincidence pulse that accompanied a valid pair of pulses was used to turn on one analog-to-digital converter for the γ-ray pulse height and another converter for the pulse which gave a measure of the γ-ray time with respect to fission. Each two-word pair defined an event that was stored sequentially on a computer disk. γ rays for times in the region of the prompt γ-ray time peak were not stored so that the disk would not fill up too rapidly. The γ-ray energy was analyzed with a 4000-channel analog-to-digital converter operating at a calibration of 1 keV per channel, and the time was analyzed with a 1024-channel converter with a calibration of 2.5 nsec per channel. A gain stabilization system was programmed into the computer to correct the channel of storage for the γ-ray energy. In this system, the outputs of two precision pulsers corresponded to γ-ray energies of 0.070 and 3.9 MeV; these outputs were fed into the preamplifier. The program corrected the signals so that the stored events from each precision pulser would always be centered at the same channel and, consequently, so would the stored events for each of the γ-ray peaks. The resulting resolution for 10-h runs with the system was about 3.0 keV.

3. RESULTS

A. γ-ray time and pulse-height data

γ-ray data were taken from about −1050 to +1160 nsec, with the time for fission designated as time zero. The γ-ray counts at negative times resulted from chance-coincidence background events, including prompt γ rays from the small fraction of fission events which were not detected because of the geometry of the source and detector. The ratio of the total γ-ray counts to the background counts was ~1.6 at 1 μsec after fission, and rapidly increased with decreasing time. The ratio of the height of a typical real peak at ~1 μsec to the background height was much greater than 1.6 because of the good resolution of the γ-ray detector. The raw ^{235}U and ^{239}Pu data were separated into 11 time groups after fission, and one time group from 900 to 555 nsec before fission

for background data. The time groups after fission were selected in roughly uniform logarithmic intervals (except for the last time group) in the interest of achieving good counting statistics for each group and minimizing the number of groups necessary to cover a large range of half-lives. These groups were 20 to 30, 30 to 45, 45 to 68, 68 to 100, 100 to 148, 148 to 215, 215 to 315, 315 to 458, 458 to 663, 663 to 958, and 958 to 1150 nsec. The background was subtracted from each of the time groups to obtain pulse-height distributions such as those shown in Figs. 4 and 5 for ^{235}U γ rays. A broad peak at 691 keV has been omitted from the figures, since this peak is due to conversion electrons following Ge(n, n') reactions in the detector. These electrons are emitted from a level with a half-life of ~0.43 μsec. The relatively few resolved peaks riding on this broad peak were analyzed, however. Measurements were made for γ-ray energies up to 4 MeV for every case, but no statistically meaningful γ rays were observed above 1314 keV for any of the spectra. For the pulse-height distribution in the time group of 68 to 958 nsec after fission, there were indications of several weak peaks above 1314 keV, but these were again not statistically positive. The counts in any such peak were on the order of 0.1, or less, of the counts in the 1314-keV peak in the time region studied. In the checkout of the experimental system, some short runs were made with ^{252}Cf in a search for γ rays with energies up to 10 MeV, and no γ rays were positively observed above 1314 keV.

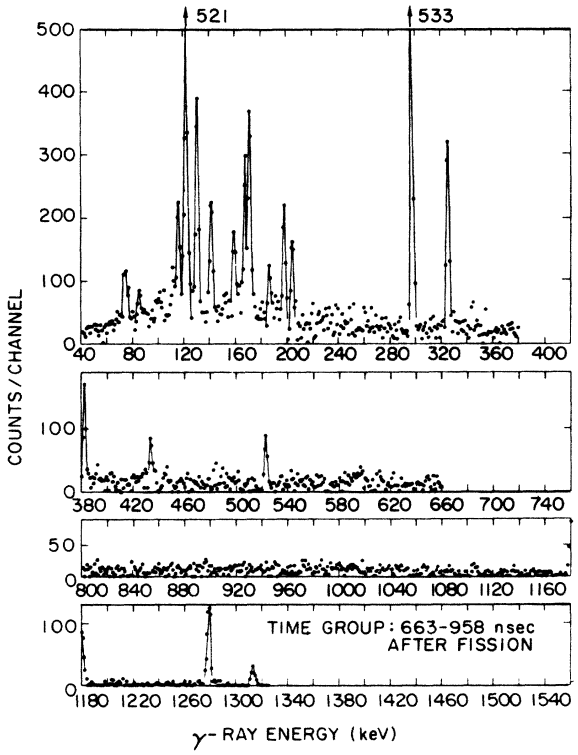

FIG. 5. Pulse-height distribution for γ rays emitted between 663 and 958 nsec after ^{235}U(n,f), uncorrected for the decrease in counts at low pulse heights due to the rejection of slow rise-time pulses.

B. Analysis of resolved γ-ray peaks for intensity and half-life

The code SAMPO (Ref. 10) was used to analyze the counts in the resolved γ-ray peaks for each of the pulse-height distributions. This code was written to provide a method capable of analyzing spectra of high complexity, including closely spaced spectral lines (multiplets) without requiring any prior knowledge of the spectral distribution. Based on the statistics of the data and the accuracy of the calibration information, over-all uncertainties were calculated and are included in the results. The parameters which define the shape of the peaks in the code were determined as a function of energy from intense and well-isolated peaks in the present delayed γ-ray data. For a peak to be finally analyzed, it had to be statistically meaningful and agree, within limits, with the shape characteristics as well.

The automatic analysis results with the SAMPO code were carefully checked by hand for several of the more prominent peaks and also for a number of smaller peaks in our delayed γ-ray pulse-height distributions; the agreement between the computer results and the hand-processed data was generally found to be very good. Under certain conditions, however, such as that of a cluster of six or more resolved but overlapping peaks, or of the case of a large peak separated from a small one by only a few channels, the results of the automatic analysis with the code were found to be unsatisfactory. In these cases the peaks were analyzed with the code by giving as additional inputs the widths of the fitting intervals and the approximate peak channels; the results then agreed well with the hand-analyzed cases.

Most of the γ-ray peaks decayed with a single half-life. Such peaks were analyzed with a least-squares program to determine the intensities and half-lives of the γ rays. The half-lives previously measured in a four-parameter experiment with ^{252}Cf at Livermore (Ref. 4) were used in the analysis of several of the present very short-lived peaks when the present data did not allow an accurate determination of the half-lives; in these cases, the uncertainties in the intensities were calculated with the assumption of no uncertainties in the half-lives. Several examples of the decay of the γ rays are shown in Fig. 6.

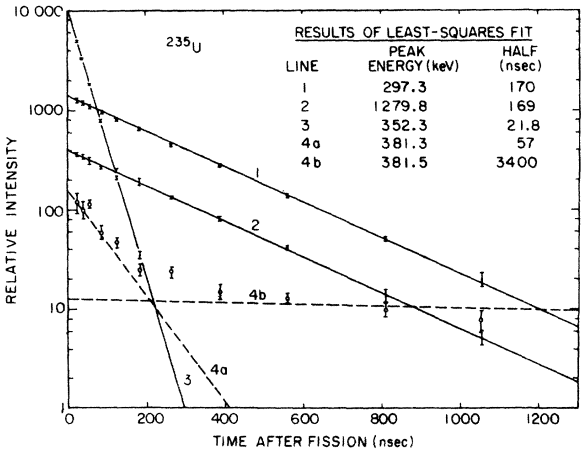

FIG. 6. Results of least-squares fit for three γ-ray peaks with a single half-life component and for one peak with two half-life components.

Even though the energy resolution of the γ-ray peaks for the measurements was ~3.0 keV, some of the γ-ray peaks from different isomers overlapped, so that some of the observed peaks decayed with a multiple half-life. This was particularly true for energies below ~200 keV. Most of these cases of overlap had half-lives that were sufficiently close in value so that the different components could not be reasonably separated by successively removing the longest-lived component. Consequently, in analyzing the multiple half-life data, the half-lives previously determined with ^{252}Cf at Livermore (Ref. 4) typically were used as input, and a least-squares fit was done to determine the intensity of each component. In the calculation of the intensity uncertainty for each component, the uncertainty contributions from the input half-lives were arbitrarily assumed to be small. The Livermore data sometimes contain three or more γ rays at almost the same energy; when two or more of these γ rays have approximately the same half-life, the half-life of the strongest γ ray was used as input for the present analysis. This approximation could produce an error in the total intensity of the two or more components with approximately the same half-life. A few of the present peaks with multiple half-lives could not be fitted with half-lives from previous data. Consequently, the uncertainties on the analyzed results for these peaks are typically larger than those for the other cases.

Three γ rays, at ~197.3, ~381.4, and ~1313.6 keV in the present data, correspond to those previously observed at this laboratory from an isomer with a half-life of 3.4 μsec (Ref. 9). The previous measurement was made with a NaI detector and gave slightly higher energies for the 3.4-μsec γ rays than the present results, but the differences are within the errors of the previous measurement. Since the previous data for this isomer extended over a time period of ~10 μsec, the half-life was determined more accurately than in the present measurement or in the Livermore ^{252}Cf measurement (Ref. 4). Consequently, the 3.4-μsec value was used for the half-life in the present analysis of these peaks. The 197.3-keV peak in the present data had components from the 3.4-μsec γ ray and from an 87-nsec background γ ray as well. The latter peak was produced from inelastic neutron scattering by the F in the LiF slow-neutron filter located between the fission sample and the Ge(Li) detector. The fast neutrons which produced this reaction were from fission events in the sample. The two half-life components for this ~197-keV peak were separated by a least-squares fit to the time-decay data, using the known half-lives as input to the calculation. The peak at ~381 keV also consisted of two components, both of which were isomers from fission; since the half-life of the shorter-lived component was not known from previous measurements, the data at later times were analyzed for the 3.4-μsec component, and then the shorter-lived component was analyzed. The results of the fit are shown in Fig. 6.

To determine absolute intensities of the γ rays, the analyzed data were corrected for (1) the measured efficiency of the Ge(Li) detector as a function of γ-ray energy, (2) the measured loss of slow rise-time pulses as a function of pulse height, and (3) the number of valid fission events. Results of the analysis of the ^{235}U and ^{239}Pu resolved γ rays for energy, E_γ, half-life, $T_{1/2}$, and intensity, I_γ, are given in Table I. The ^{235}U and ^{239}Pu γ-ray peaks which appear to have the same energy and half-life are given on the same line; uncertainties on the energies are ~±0.4 keV. The half-life uncertainty, $\pm\Delta T_{1/2}$, and intensity uncertainty, $\pm\Delta I_\gamma$, given in the table for particular γ rays are from the peak analysis and least-squares fitting and do not include the uncertainty in the Ge(Li) detector efficiency and other uncertainties which could affect the absolute intensity. These possible systematic uncertainties are estimated to be ~±10% for ^{235}U and ~±15% for ^{239}Pu for γ rays with energies above ~130 keV. Below 130 keV the systematic uncertainties are somewhat larger because of the larger uncertainties in the Ge(Li) detector efficiency. The larger uncertainty for the ^{239}Pu is due to the degradation of the fission-fragment detectors from radiation damage during the experiment and the resultant loss of some low-energy fission pulses. The in-

TABLE I. Delayed γ-ray resolved peaks observed in the present ^{235}U and ^{239}Pu measurements. For comparison the Livermore ^{252}Cf results (Ref. 4) are shown for those γ rays which appear to correspond in energy and half-life to the peaks observed from ^{235}U or ^{239}Pu. For the present results, a reference is given if the half-life was taken from previous research. The uncertainties given for the present ^{235}U and ^{239}Pu γ-ray intensities do not include possible systematic uncertainties of ~±10 and ~±15%, respectively, for energies above ~130 keV and somewhat larger values below 130 keV.

Present results												Livermore results ^{252}Cf			
^{235}U						^{239}Pu									
E_γ (keV)	$T_{1/2}$ (nsec)	$\pm\Delta T_{1/2}$ (%)	$T_{1/2}$ Ref.	I_γ (photons/fission)	$\pm\Delta I_\gamma$ (%)	E_γ (keV)	$T_{1/2}$ (nsec)	$\pm\Delta T_{1/2}$ (%)	$T_{1/2}$ Ref.	I_γ (photons/fission)	$\pm\Delta I_\gamma$ (%)	E_γ (keV)	A [a]	$T_{1/2}$ (nsec)	I_γ [b] (photons/fission)
85.0	15.	20		0.0118	50	85.3	15.	18		0.024	50	85.6 85.7	105^{+1}_{-0} 133^{+0}_{-1}	16 12	0.0012 0.0026
85.1 [c]	135.	30		0.0048	50	85.5 [c]	135.	27		0.0069	48				
91.3	120.		4	0.0025	29	91.3	120.		4	0.001 69	26	90.0 91.2	108^{+1}_{-0} 132 ± 0	120 120	0.0022 0.000 75
91.3	15.		4	0.0021	35	91.3	15.		4	0.0039	35	90.2 90.5 91.5	108 ± 0 142 ± 0 101^{+0}_{-1}	15 15 19	0.0013 0.000 89 0.000 76
						102.8	15.		4	0.0038	14	102.8 103.5	105 ± 0 111^{+0}_{-1}	15 14	0.0038 0.0059
						102.8	200.		4	0.0099	29	103.2	150^{+0}_{-1}	200	0.0011
						106.6	20.		4	0.0018	60	105.0 106.0	146 ± 2 142 ± 2	20 20	0.0023 0.0029
109.1	11.9	10		0.0095	40	109.4	10.7	12		0.0079	40				
115.3	175.	4		0.0103	7	115.3	175.	5		0.0089	7	115.0	134 ± 0	162	0.0061
121.6	360.		4	0.0101	7	121.4	360.		4	0.0094	7	121.4	99^{+1}_{-0}	360	0.0048
121.8	22.		4	0.002 19	15	121.7	22.		4	0.0034	17	122.0	99^{+1}_{-0}	22	0.0025
125.0	81.6	14		0.002 16	14	125.0	79.2	16		0.0033	15	125.1	134 ± 0 [d]	115	0.001 76
130.5	375.	3		0.0089	9	130.1	340.		4	0.0077	25	129.8	99^{+1}_{-0}	340	0.0029
						130.5	19.		4	0.0012	30	130.5	146 ± 0	19	0.0032
141.5	360.		4	0.004 15	5	141.3	360.		4	0.0025	11	140.9	96^{+1}_{-0}	360	0.000 84
142.3	55.		4	0.0368	4	142.1	55.		4	0.0188	4	140.9 142.0	104 ± 0 91^{+1}_{-0}	62 55	0.0016 0.0036
						153.8	143.	12		0.0021	11	153.6	108 ± 0	110	0.0077
162.4	97.1	4		0.0073	5							163.0 163.5	133^{+0}_{-1} 152 ± 0	110 82	0.0018 0.000 114
167.4	240.		4	0.0032	15	167.1	240.		4	0.000 42	12	167.1	96^{+1}_{-0}	240	0.0015
167.7	13.		4	0.0072	30	167.7	13.		4	0.0028	30	167.7	146^{+1}_{-0}	13	0.0073
169.	1100.		4	0.0027	21	170.5	1100.		4	0.0039	19	170.5	98 ± 0	1100	0.0020
181.2	127.	20		0.0011	36	181.0	127.	20		0.0024	38				
181.5	28.0	10		0.0013	30	181.6	28.0	10		0.0026	32				
186.5	1166.	15		0.0017	30	186.1	1000.	30		0.0013	42	186.4	98 ± 1 [d]	650	0.0005
191.7	115.	10		0.0023	25	191.8	162.	33		0.0010	40	191.1	94^{+0}_{-1}	110	0.000 29

TABLE I *(Continued)*

Present results											Livermore results			
^{235}U						^{239}Pu					^{252}Cf			
E_γ (keV)	$T_{1/2}$ (nsec)	$\pm\Delta T_{1/2}$ (%)	$T_{1/2}$ Ref.	I_γ (photons/fission)	$\pm\Delta I_\gamma$ (%)	E_γ (keV)	$T_{1/2}$ (nsec)	$\pm\Delta T_{1/2}$ (%)	$T_{1/2}$ Ref.	I_γ (photons/fission)	$\pm\Delta I_{1/2}$ (%)	E_γ (keV)	A [a]	$T_{1/2}$ (nsec)	I_γ [b] (photons/fission)
197.3	3400.		9	0.0082	15	197.3	3400.		9	0.0152	15	197.3	136	2800	0.0060
204.0	3000.		4	0.0064	9	204.0	3000.		4	0.0034	11	204.0	98 ± 1	3000	0.0013
204.3	24.		4	0.0408	15	204.2	24.		4	0.0238	15	204.3	95 ± 2	24	0.0062
217.4	94.	10		0.0036	10	217.3	128.	25		0.0015	25	217.2	93 ± 0	70	0.000 44
228.8	16.5	4		0.0014	25										
276.1	7.6	15		0.0065	60	276.0	7.6		e	0.0039	80	276.5	91	6	0.000 43
283.8	8.		4	0.0040	80	283.5	8.		4	0.0040	80	283.9	147^{+1}_{-0}	8	0.0064
288.1	12.6	19		0.0015	30	288.2	12.9	10		0.001 94	30	288.2	146 ± 0	17	0.0029
297.3	170.	3		0.0297	5	297.2	183.	5		0.0226	5	296.9	134 ± 0	162	0.0103
314.3	8.2	10		0.0055	60	314.1	8.7	10		0.0082	60	314.4	138^{+0}_{-1}	9	0.0039
325.3	555.	5		0.0053	6	324.9	578.	18		0.0031	19	324.5	135 ± 0	570	0.0031
						330.8	26.	30		0.028	33				
						330.8	168.	70		0.000 21	75				
339.8	86.	6		0.001 84	8	339.5	79.	14		0.000 77	17				
						343.2	674.	36		0.0011	37				
352.3	21.8	5		0.0326	20	352.1	22.6	5		0.0181	20	352.3	95 ± 0	21	0.0046
381.3	57.	7		0.0012	19	381.3	57.	20		0.000 95	30				
381.5	3400.		9	0.0059	22	381.1	3400.		9	0.0176	20	380.7	136	3400	0.0073
387.5	119.	10		0.0010	30	387.2	115.	3		0.0030	16	387.1	135^{+0}_{-1}	110	0.000 82
400.1	7.8	10		0.0059	80	400.1	8.1	10		0.0075	80	400.2	138^{+0}_{-1}	9	0.0037
412.7	18.3	6		0.0034	25	412.1	22.4	9		0.0020	25				
415.7	24.5	6		0.0024	20	415.4	20.2	13		0.0021	20	415.6	99^{+1}_{-0}	16	0.000 51
426.8	15.4	7		0.0028	30	426.4	15.7	6		0.0028	30	426.8	100 ± 1	16	0.000 88
433.0	1960.	48		0.0026	52	432.3	1450.	55		0.0038	60				
						444.7	215.	5		0.001 11	15				
444.8	50.	10		0.000 43	27										
444.8	520.	15		0.000 99	29										
454.2	19.2	16		0.001 11	25	454.2	15.5	17		0.001 25	25				
461.2	161.	14		0.000 62	21	461.4	90.	5		0.000 75	15				
522.4	382.	11		0.002 12	17										
536.3	22.7	10		0.001 78	16	535.5	28.9	10		0.001 61	15				
575.8	16.8	10		0.002 26	30	576.2	19.8	16		0.001 47	30				
589.8	68.4	6		0.001 83	12	590.3	100.	50		0.0013	52				
614.2	17.3	10		0.0194	30	614.2	17.3	10		0.0179	30	614.2	100 ± 0	20	0.0034
619.6	96.	5		0.001 87	10										
648.7	165.	17		0.001 46	21	648.2	104.	32		0.000 76	34				

TABLE I *(Continued)*

Present results												Livermore results			
^{235}U						^{239}Pu						^{252}Cf			
E_γ (keV)	$T_{1/2}$ (nsec)	$\pm\Delta T_{1/2}$ (%)	$T_{1/2}$ Ref.	I_γ (photons/fission)	$\pm\Delta I_\gamma$ (%)	E_γ (keV)	$T_{1/2}$ (nsec)	$\pm\Delta T_{1/2}$ (%)	$T_{1/2}$ Ref.	I_γ (photons/fission)	$\pm\Delta I_\gamma$ (%)	E_γ (keV)	A [a]	$T_{1/2}$ (nsec)	I_γ [b] (photons/fission)
746.7	132.	37		0.000 93	39										
770.4	2060.	60		0.0026	64	770.1	1050.	35		0.0025	37				
774.6	46.5	7		0.001 18	12	774.8	49.9	12		0.0015	16				
810.6	102.	4		0.001 34	16										
815.4	15.0	10		0.000 74	40										
817.5	117.	20		0.000 70	35										
						840.3	129.	25		0.000 84	40				
968.6	28.2	14		0.001 44	17	969.5	28.8	6		0.001 97	10				
974.7	120.	5		0.002 39	8	975.2	69.	35		0.0020	30				
						975.2	278.	35		0.0027	30				
998.4	96.	11		0.000 92	35										
1025.3	20.5	8		0.002 11	20	1025.9	20.9	8		0.001 46	20				
1086.5	21.6	12		0.001 29	25	1087.1	19.7	10		0.001 45	25				
1103.4	113.	5		0.0045	7	1103.7	111.	4		0.0062	6				
1150.7	110.	5		0.0041	5	1151.1	124.	9		0.0061	9	1151.6	134^{+0}_{-1}	90	0.0021
1180.8	612.	10		0.0054	12	1180.8	499.	13		0.0031	13	1181.0	135^{+0}_{-1}	670	0.0030
1221.5	31.	50		0.0021	60	1221.4	15.2	40		0.0042	60	1221.0	137^{+2}_{-1}	6	0.0073
1279.8	169.	3		0.0235	5	1279.8	179.	4		0.0177	5	1279.8	134 ± 0	164	0.0126
1313.9	3400.		9	0.0095	30	1313.4	3400.		9	0.0156	35	1313.3	136	3000	0.0057

[a] Because of the large number of γ rays at low energies, the assignment of the ^{235}U and ^{239}Pu peaks to the A values given for the ^{252}Cf peaks is not positive below ~200 keV.

[b] See Sec. 4 A for a comparison of the Livermore (Ref. 4) results for ^{252}Cf and the present results for a number of γ rays for ^{252}Cf.

[c] This peak does not correspond to the peak with approximately the same energy and same half-life observed in the Livermore data (Ref. 4), since the Livermore peak is from $A \approx 108$, and the ^{235}U and ^{239}Pu fission fragment yields for this mass number are significantly lower than the observed yields.

[d] Since the error bars on the ^{235}U and ^{239}Pu half-lives do not overlap the value of the ^{252}Cf half-life, the γ rays in ^{235}U and ^{239}Pu may be from a different mass number.

[e] The half-life was taken from the present ^{235}U data.

tensity uncertainties for the γ rays with very short half-lives are particularly large, since a small uncertainty in the value of the half-life produces a large uncertainty in intensity in these cases. Several peaks with half-lives too short to be analyzed, or with poor statistics, are not given in the table; these peaks were analyzed with the unresolved γ rays, as discussed later.

For comparison with the present data, the Livermore ^{252}Cf results are shown in Table I for those γ rays which appear to correspond in both energy and half-life to the peaks observed from ^{235}U and ^{239}Pu. The value of the mass number A for the fragment emitting each γ ray is given for the ^{252}Cf data along with the half-life, energy, and intensity of the γ ray. In Sec. 4A the Livermore intensities and half-lives are compared with those from the present experiment for a number of γ rays from ^{252}Cf. A number of γ rays observed in the present measurements were also previously observed by Ajitanand in measurements with ^{252}Cf (Ref. 5).

Since the prompt neutrons from fission can produce inelastic scattering in material in the region of the Ge(Li) detector, isomeric γ rays can be produced that are related in time to the detected fission events, and therefore appear as backgrounds for the delayed γ-ray events. In the Livermore ^{252}Cf measurement, such backgrounds could be positively identified, since the background γ rays would not be associated with a particular mass number A, but would appear for all mass values. In the present experiment, the γ rays which did not correspond to those observed from ^{252}Cf at Livermore were checked to determine if they were produced from inelastic neutron scattering. In one check a PuBe source was located near the detector system, and the detected γ rays were compared to the delayed γ-ray spectra to see if any peaks corresponded. In a second check, the ratios of the γ-ray intensities per fission for ^{235}U, ^{239}Pu, and the present ^{252}Cf data were compared for each peak in question to determine if the ratios agreed with the known ratios of prompt neutrons per fission, ν_p. If the ratios were in rough agreement with the ν_p values for a given peak, then the peak could possibly be caused by the decay of a short-lived isomer produced by inelastic scattering of the prompt neutrons. The studies showed that a 197-keV, 87-nsec peak was a background γ ray from $^{19}F(n,n')\gamma$ reactions, as described earlier.

C. Analysis of continuum γ rays

Since a large number of delayed γ rays with weak intensities could form a continuum of unresolved γ rays that would not be analyzed with the peak-analysis procedure given above, the pulse-height distributions were further analyzed to obtain the total γ-ray energy per fission versus delay time. This analysis included a number of resolved γ-ray peaks that were not included in Table I because the peaks had half-lives too short to analyze or had poor statistics. The pulse-height distributions were first grouped into five time groups of 20 to 45, 45 to 100, 100 to 215, 215 to 458, and 458 to 958 nsec after fission. The tabulated (Table I) γ-ray peaks and their associated Compton distributions were then subtracted from the five pulse-height spectra, and the resulting spectra were unfolded with the FERDOR code (Ref. 11) to determine the continuum spectra for the five time regions. In the analysis, corrections were made for the rejection of slow rise-time pulses by the fast-timing circuitry. In removing the γ-ray peaks, the least-squares fit to the time-decay data for each γ-ray peak was used, and not the peak area determined from the particular time group being processed. In this way, peak-area variations from statistics and from uncertainties in the height of the Compton events beneath each peak were smoothed. Also, with this method the short-lived γ-ray peaks could be subtracted from late time groups, even though the peaks were not readily obvious in the late-time pulse-height distribution. This was similarly true for the long-lived peaks in the analysis of the early-time groups. The analyzed continuum spectra were grouped into five energy bins from 140 to 1340 keV. Because of the various subtractions, the input data for the unfolding was relatively unsmooth. To prevent negative-going oscillations in the calculational output, a 40% wide window function was used in the analysis. Although this is wider than desirable, the unfolding results obtained with other window functions indicated that the over-all errors introduced in these spectra by this window function were not large. The continuum in the region of the broad 691-keV conversion-electron background peak from Ge was estimated by a straight line joining the continuum below and above the peak.

Some of the observed continuum was from time slewing of the prompt γ rays. The effect of the time slewing as a function of γ-ray energy was determined from sets of data similar to those shown in Fig. 3, and the 20- to 45- and 45- to 100-nsec continuum data were then corrected before the unfolding. Time slewing had a negligible effect for later time bins.

The total intensities and energies of delayed γ rays from ^{235}U and ^{239}Pu, as determined by adding the resolved γ-ray peak results to the unfolded

continuum data discussed above, are given in Tables II and III, respectively. The uncertainties given in these tables include the statistical uncertainties in the data and the uncertainties in the continuum analysis that arise from subtracting the Compton distributions associated with resolved higher-energy γ rays, from the time-slewing corrections for the prompt γ rays, and from the relatively wide window function used in the unfolding. The uncertainties are relatively large at early times where the uncertainties in the time-slewing corrections for the continuum results are correspondingly large. In addition to the uncertainties given in Tables II D and III D, ~±10 and ~±15% systematic uncertainties exist on the ^{235}U and ^{239}Pu data, respectively; these uncertainties are described in Sec. 3 B. The ratios of the energy of the resolved γ rays to the energy of the total (resolved and continuum) γ rays are also given in Tables II and III. Most of the energy observed in this experiment is in the resolved peaks, as indicated by ratios of 0.80 and 0.76 for ^{235}U and ^{239}Pu, respectively, for γ rays above 140 keV and for the time interval of 20 to 958 nsec after fission.

4. DISCUSSION

A. Comparison of selected ^{252}Cf resolved γ-ray results with previous results

To check the consistency between the results for the present experiment and the previous Livermore ^{252}Cf experiment (Ref. 4), the present ^{252}Cf data were analyzed for the intensities and half-lives of some of the strong resolved γ rays. To check further on the consistency between experiments, the present data were also analyzed for some resolved γ rays previously observed to be in cascade (Refs. 4, 9); in some of these cases, half-lives from previous data were used as inputs for the present intensity determinations. A comparison of the results is given in Table IV. The errors shown in Table IV for the Livermore in-

TABLE II. Grouped values for ^{235}U isomeric γ rays.

Energy group (keV)	Time group (nsec) 20–45	45–100	100–215	215–458	458–958	20–958
A. Number of resolved and continuum γ rays per fission						
140–380	4.5×10^{-2}	4.0×10^{-2}	2.9×10^{-2}	1.85×10^{-2}	1.11×10^{-2}	1.43×10^{-1}
380–620	1.63×10^{-2}	1.06×10^{-2}	5.9×10^{-3}	4.1×10^{-3}	2.7×10^{-3}	4.0×10^{-2}
620–860	3.1×10^{-3}	3.0×10^{-3}	2.6×10^{-3}	1.93×10^{-3}	1.32×10^{-3}	1.19×10^{-2}
860–1100	3.9×10^{-3}	2.7×10^{-3}	2.1×10^{-3}	1.03×10^{-3}	6.1×10^{-4}	1.04×10^{-2}
1100–1340	5.4×10^{-3}	7.6×10^{-3}	1.00×10^{-2}	9.9×10^{-3}	6.0×10^{-3}	7.0×10^{-3}
140–1340	7.4×10^{-2}	6.4×10^{-2}	4.91×10^{-2}	3.5×10^{-2}	2.2×10^{-2}	2.4×10^{-1}
B. Energy (keV) per fission for the resolved and continuum γ rays						
140–380	10.8	9.2	6.4	4.4	2.6	33.
380–620	8.5	5.5	3.0	2.0	1.26	20.4
620–860	2.9	2.2	2.0	1.39	.97	9.9
860–1100	3.9	2.7	2.1	1.02	.59	10.3
1100–1340	6.5	9.3	12.4	12.2	7.5	48.
140–1340	33.	28.9	25.9	21.0	12.9	121.
C. Ratio of energy of the resolved γ rays to the energy of the resolved and continuum γ rays						
140–380	0.89	0.91	0.89	0.94	0.94	0.90
380–620	0.73	0.71	0.54	0.53	0.70	0.67
620–860	0.27	0.47	0.57	0.66	0.55	0.47
860–1100	0.47	0.64	0.54	0.67	0.32	0.54
1100–1340	0.75	0.90	0.92	0.95	0.97	0.91
140–1340	0.71	0.81	0.81	0.88	0.89	0.80
D. Uncertainties (%) for the number of γ rays per fission and the energy per fission[a]						
140–380	10	7	5	4	5	
380–620	17	12	10	10	6	
620–860	36	16	13	10	14	
860–1100	24	11	16	13	40	
1100–1340	10	4	4	3	3	

[a] The uncertainties do not include possible systematic uncertainties of ~±10%.

tensities are the total errors. In most cases, the percent error on the half-life for the Livermore results was estimated to be roughly the same as the percent error on the intensity (Ref. 4). The half-lives which were calculated independently in the two experiments typically agree within the combined errors of the experiments. Also, most of the intensities agree within the combined error bars, including the systematic uncertainties. For all of the γ rays in Table IV except the 3.4-μsec γ rays, which have relatively large intensity uncertainties due to the long half-life, the Livermore intensities are on the average ~14% lower than the present intensities. This is slightly less than the sum of the estimated systematic uncertainties for both experiments.

B. Comparison of ^{235}U, ^{239}Pu, and ^{255}Cf results

Differences in the isomeric yields for the three cases of fission are expected because of the difference in the mass-yield curves, as well as the difference in the atomic number distribution for a given mass. For the thermal-neutron fission of ^{235}U and ^{239}Pu and for spontaneous fission of ^{252}Cf, the shift in the lower peak of the mass-yield curve from one case of fission to another is much more significant than that in the upper peak, since the lower peak is at mass number $A \sim 96$, ~102, and ~109, respectively and the upper peak is at ~139, ~138, and ~142, respectively.

As indicated in Table I, many of the same resolved γ rays were observed in the present experiment on ^{235}U and ^{239}Pu and in the previous ^{252}Cf experiment at Livermore (Ref. 4). A total of 80 γ-ray peaks with different energies and half-lives was observed in the ^{235}U and ^{239}Pu data. Of these peaks the same 58 were observed in both ^{235}U and ^{239}Pu, and the same 37 were observed in the present ^{235}U and ^{239}Pu results and the previous ^{252}Cf results (Ref. 4). Thirty-seven γ-ray peaks which

TABLE III. Grouped values for ^{239}Pu isomeric γ rays.

Energy group (keV)	Time group (nsec) 20–45	45–100	100–215	215–458	458–958	20–958
	A. Number of resolved and continuum γ rays per fission					
140–380	3.6×10^{-2}	3.0×10^{-2}	1.96×10^{-2}	1.35×10^{-2}	1.00×10^{-2}	1.09×10^{-1}
380–620	1.45×10^{-2}	9.1×10^{-3}	5.9×10^{-3}	4.9×10^{-3}	3.4×10^{-3}	3.8×10^{-2}
620–860	4.0×10^{-3}	2.7×10^{-3}	2.5×10^{-3}	1.83×10^{-3}	1.72×10^{-3}	1.27×10^{-2}
860–1100	4.1×10^{-3}	3.2×10^{-3}	2.4×10^{-3}	2.2×10^{-3}	1.40×10^{-3}	1.34×10^{-2}
1100–1340	5.8×10^{-3}	7.3×10^{-3}	9.5×10^{-3}	9.3×10^{-3}	6.0×10^{-3}	3.8×10^{-2}
140–1340	6.4×10^{-2}	5.3×10^{-2}	4.0×10^{-2}	3.2×10^{-2}	2.2×10^{-2}	2.1×10^{-2}
	B. Energy (keV) per fission for the resolved and continuum γ rays					
140–380	9.4	7.6	4.7	3.3	2.4	27.4
380–620	7.5	4.6	2.9	2.2	1.53	18.7
620–860	3.0	2.0	1.84	1.39	1.29	9.4
860–1100	4.1	3.2	2.4	2.2	1.36	13.2
1100–1340	7.1	8.9	11.5	11.5	7.5	46.
140–1340	31.	26.3	23.2	20.5	14.0	115.
	C. Ratio of energy of the resolved γ rays to the energy of the resolved and continuum γ rays					
140–380	0.91	0.94	0.90	0.90	0.90	0.92
380–620	0.74	0.73	0.50	0.49	0.70	0.67
620–860	0.15	0.33	0.38	0.41	0.38	0.30
860–1100	0.47	0.58	0.53	0.43	0.46	0.50
1100–1340	0.74	0.87	0.89	0.93	0.93	0.88
140–1340	0.70	0.79	0.77	0.79	0.80	0.76
	D. Uncertainties (%) for the number of γ rays per fission and the energy per fission[a]					
140–380	9	5	7	4	3	
380–620	16	11	10	10	15	
620–860	42	21	19	18	19	
860–1100	24	13	17	23	32	
1100–1340	11	6	6	4	6	

[a]The uncertainties do not include possible systematic uncertainties of ~±15%.

were not in the previous ^{252}Cf data (Ref. 4) were observed in either the ^{235}U or ^{239}Pu results. The most significant yield changes for particular γ rays observed in all three cases of fission are for fragments in the region of the lower hump of the mass-yield curve. Some of the γ rays observed in previous measurements (Ref. 4) on ^{252}Cf are missing in the present ^{235}U and ^{239}Pu data because they arise from fission fragments with A values having low yields for ^{235}U and ^{239}Pu, or because they are weak and masked by other γ rays in the same energy region.

The energies and half-lives of corresponding peaks from the different cases of fission typically agree within the total uncertainties. The comparison between the present ^{235}U and ^{239}Pu results and the previous ^{252}Cf results are not completely positive below ~200 keV due to the number of γ rays overlapping in energy. Above 400 keV all of the γ rays observed from ^{252}Cf at Livermore (Ref. 4) were observed in the present ^{235}U and ^{239}Pu results, except for the 445.0-keV transition with a 14-nsec half-life from $A = 147$ (Ref. 4). The mass-yield curves indicate that this isomer should, indeed, be weaker in ^{235}U and ^{239}Pu than in ^{252}Cf. The present ^{235}U and ^{239}Pu results show a significant number of isomers above 400 keV that were not observed from ^{252}Cf. Most of these new γ rays are probably again due to differences in the mass-yield curves. In several cases, though, the present ^{252}Cf data show γ rays which correspond to those from ^{235}U and ^{239}Pu, but which were not observed in the Livermore ^{252}Cf results. These cases include γ rays at ~775, 975, and 1103 keV in the present data, with absolute intensities of very roughly 0.0012, 0.0016, and 0.000 85 per ^{252}Cf fission event, respectively. These γ rays were probably observed in the present experiment because the Ge(Li) detector is significantly larger than that used in the Livermore experiment, and consequently the present detector efficiency does not drop off nearly as rapidly with energy. The measured half-lives shown in Table I for the 1221-keV γ ray do not agree within the assigned uncertainties, even though these uncertainties are large for this case. The 1221-keV γ ray may possibly originate from two isomers with different half-lives.

The γ rays observed at Livermore for ^{252}Cf fission fragments had energies and half-lives corresponding mainly to $E1$, $M1$, or $E2$ transitions, either allowed or K forbidden by a few units (Ref. 4). Since many of the γ rays from ^{235}U and ^{239}Pu fission fragments are identical to those from ^{252}Cf fission fragments, and since the new γ rays from ^{235}U and ^{239}Pu have half-lives and energies in the same region, the same conclusions concerning multipolarity apply to the γ rays from ^{235}U and ^{239}Pu fission fragments.

The total energy of the resolved γ rays when integrated over all time is 163 keV/fission for the ^{235}U results and 164 keV/fission for the ^{239}Pu results. These results do not include the continuum contribution. The two values are closer than would be expected from the large intensity differences in specific γ rays; particular time and energy groups show much larger changes. The corresponding yield for ^{252}Cf is ~82 keV per fission; this was obtained from the Livermore measurements (Ref. 4) by including γ rays in the same half-life range (i.e., $\geq$8 nsec and also the 276.5- and 1221-keV γ rays). The present data for only the resolved γ rays give 125 and 119 keV/fission for ^{235}U and ^{239}Pu, respectively, from 10 to 2000 nsec. For comparison, the Livermore ^{252}Cf experiments yielded a total of 58 keV/fission in the peak data from 10 to 2000 nsec (Ref. 12). Any possible systematic difference in the results from

TABLE IV. Comparison of selected ^{252}Cf delayed γ rays from present measurement with those from Livermore measurement (Ref. 4). The errors for the present results do not include systematic uncertainties of ~±10%.

Present results						Livermore results				
E_γ (keV)	$T_{1/2}$ (nsec)	$\pm\Delta T_{1/2}$ (%)	$T_{1/2}$ Ref.	I_γ (photons/fission)	$\pm\Delta I_\gamma$ (%)	E_γ (keV)	A	$T_{1/2}$ (nsec)	I_γ (photons/fission)	$\pm\Delta I_\gamma$ (%)
115.2	162.		4	0.0058	9	115.0	134±0	162	0.0061	7
176.3	89.	5		0.0041	10	176.2	108^{+1}_{0}	110	0.0031	7
197.4	3400.		9	0.0092	15	197.3	136	2800	0.0060	8
297.3	168.	3		0.0150	5	296.9	134±0	162	0.0103	7
325.3	513.	5		0.0042	15	324.5	135±0	570	0.0031	8
352.3	23.1	5		0.0054	20	352.3	95±0	21	0.0046	7
381.6	3400.		9	0.0086	20	380.7	136	3400	0.0073	8
1150.6	103.1	6		0.0031	9	1151.6	134^{+0}_{-1}	90	0.0021	11
1180.5	474.	12		0.0029	10	1181.0	135^{+0}_{-1}	670	0.0030	13
1279.9	167.	3		0.0114	5	1279.8	134±0	164	0.0126	9
1313.4	3400.		9	0.0086	35	1313.3	136	3000	0.0057	24

the two laboratories, as discussed in Sec. 4A, is much smaller than the energy difference between the ^{252}Cf results and the ^{235}U or ^{239}Pu results. The total energy of the cascade γ rays for the 3.4-μsec and 170-nsec isomers, which will be discussed in Sec. 4C is ~58, 64, and 37 keV/fission for ^{235}U, ^{239}Pu, and the present ^{252}Cf results, respectively. The values show that these isomers account for a significant percentage of the total peak energy observed (36% in the case of ^{235}U) and that changes in the yields of several isomers can cause a significant effect on the total energy per fission. Also, roughly 40% of the total energy of the resolved γ rays, integrated over all times, is from γ rays in the 1100- to 1340-keV region for both ^{235}U and ^{239}Pu.

In the 45- to 100-nsec time region after fission, most of the energy is from the 140- to 620-keV and the 1100- to 1340-keV regions, with relatively little energy from the 620- to 1100-keV interval. In the 458- to 958-nsec time region, most of the energy is from the 1100- to 1340-keV region, and the low-energy γ rays have decreased in importance.

C. Cascade γ rays from the same isomeric state

The previous ^{252}Cf measurements at Livermore (Ref. 4), and the previous ^{235}U and ^{239}Pu measurements at this laboratory (Ref. 9) for times greater than 2 μsec after fission, indicate cases in which the γ rays decay in cascade from the same isomeric state. The determination of the mass number A of the fission fragment for each γ ray observed in the ^{252}Cf experiment (Ref. 4) was particularly valuable in identifying cascade members. Table V gives cascades which were identified in the present experiment on the basis of the previous determinations of A (Ref. 4), similar half-lives, and similar values of the intensities. Also, the previous ^{252}Cf data (Ref. 4) are given in the table for those cascades corresponding to the present ^{235}U and ^{239}Pu cascades. The γ rays which are very likely in cascade are connected with a solid line located to the left of the ^{235}U γ-ray energies listed in Table V, and the γ rays which are possibly in cascade are connected by a dashed line. The significant intensity difference in some members of suggested cascades is due to the different internal conversion coefficients of some of the transitions.

The intensity ratios for a particular set of cascade γ rays are typically expected to be the same for different cases of fission. By comparing the ratios, it appears that the following pairs of γ rays, which previous data (Ref. 4) indicated could possibly be in cascade, are probably not: 140.9 keV (360 nsec), 167.1 keV (240 nsec); 122.0 keV (22 nsec), 415.6 keV (16 nsec); and 85.6 keV (16 nsec), 102.8 keV (15 nsec). The energies and half-lives are from the previous data (Ref. 4). These conclusions are not definite, because of the large number of overlapping γ rays at low energies in the present experiment. The previously suggested cascade (Ref. 4) of 426.8 keV (16 nsec) and 614.2 keV (20 nsec) is unlikely because the difference in the two γ-ray intensities for each of the three cases of fission appears too large to be explained by possible values of the internal conversion coefficient; however, a more complicated decay scheme from the possible isomeric state might explain the intensity difference.

Several other cascades which were suggested in previous results (Ref. 4), but which are not given in Table V, were possibly identified as such in the present data. However, the differences in the half-lives and the intensities for the γ rays in each candidate cascade make the identification of these γ-ray groups as definite cascades less positive than the identification of the cases given in the table.

John *et al.* at Livermore (Ref. 4) suggest that the ~170-nsec isomer is from $^{134}_{52}Te_{82}$. An extrapolation of the energies of the first 2+ states for nuclei with $N=82$ and $Z=58$, 56, and 54 to $Z=52$ indicates a level at 1.28 MeV for $^{128}_{52}Te_{82}$ (Ref. 4), and a level at ~1.3 MeV has been predicted in theoretical calculations (Ref. 13). These energies are consistent with the energy of the 1279.8-keV γ ray. The γ-ray decay sequence for the ~170-nsec isomer is probably 115.3, 297.2, and 1279.8 keV. If one assumes an $E2$ transition for the 115.3-keV γ ray, and then combines the resulting internal conversion coefficient of 0.97 for both the K and L shells with the γ-ray intensities, the total transitions per fission for the ^{235}U, the ^{239}Pu, the present ^{252}Cf, and the Livermore ^{252}Cf results are 0.0203, 0.0175, 0.0114, 0.0120, respectively. These values roughly agree with the intensities of the 297.2- and 1279.8-keV γ rays which are part of the same cascade.

The 3.4-μsec isomer was previously observed at this laboratory (Ref. 9) for times greater than 2 μsec after the neutron fission of ^{235}U and ^{239}Pu, as discussed in Sec. 3B. John *et al.* (Ref. 4) also saw this cascade in the Livermore ^{252}Cf data, and they suggest that this isomer is from $^{136}_{54}Xe_{82}$. This isotope has levels at 1.30 (2+), 1.68, and 1.89 MeV, as determined by proton inelastic scattering measurements (Ref. 14). These levels agree with a γ-ray decay sequence of 197.3, 381.4, and 1313.6 keV. In measurements of the γ rays following the β decay of ^{136}I, γ rays at 197.7±0.3, 381.7±0.2, and 1313.2±0.8 keV were observed

TABLE V. Cascade delayed γ rays from the same isomeric state. The ^{235}U and ^{239}Pu data are from the present experiment. The ^{252}Cf data are from the Livermore experiment (Ref. 4), except the cases noted by a footnote to be from the present experiment. Systematic uncertainties in the photon intensities of ~±10%, ~±15%, and ~±10% are not included in the present results for ^{235}U, ^{239}Pu, and ^{252}Cf, respectively.

^{235}U					^{239}Pu					^{252}Cf				
E_γ (keV)	$T_{1/2}$ (nsec)	$\pm\Delta T_{1/2}$ (%)	I_γ (photons/fission)	$\pm\Delta I_\gamma$ (%)	E_γ (keV)	$T_{1/2}$ (nsec)	$\pm\Delta T_{1/2}$ (%)	I_γ (photons/fission)	$\pm\Delta I_\gamma$ (%)	E_γ (keV)	A	$T_{1/2}$ (nsec)	I_γ (photons/fission)	$\pm\Delta I_\gamma$ (%)
217.4	94.	10	0.0036	10	217.3	128.	25	0.0015	25	217.2	93 ± 0	70	0.000 44	10
191.7	115.	10	0.0023	25	191.8	162.	33	0.0010	40	191.1	94^{+0}_{-1}	110	0.000 29	13
204.3	24.		0.0408	15	204.2	24.		0.0238	15	204.3	95 ± 2	24	0.0062	12
352.3	21.8	5	0.0326	20	352.1	22.6	5	0.0181	20	352.3	95 ± 0	21	0.0046	7
121.6	360.		0.0101	7	121.4	360.		0.0094	7	121.4	99^{+1}_{-0}	360	0.0048	10
130.5	375.	3	0.0089	9	130.1	340.		0.0077	25	129.8	99^{+1}_{-0}	340	0.0029	15
115.3	175.	4	0.0103	7	115.3	175.	5	0.0089	7	115.2 [a]		162	0.0058	9
										115.0	134 ± 0	162	0.0061	7
297.3	170.	3	0.0297	5	297.2	183.	5	0.0226	5	297.3 [a]		168	0.0150	5
										296.9	134 ± 0	162	0.0103	7
1279.8	169.	3	0.0235	5	1279.8	179.	4	0.0177	5	1279.9 [a]		167	0.0114	5
										1279.8	134 ± 0	164	0.0126	9
325.3	555.	5	0.0053	6	324.9	578.	18	0.0031	19	324.5	135 ± 0	570	0.0031	8
1180.8	612.	10	0.0054	12	1180.8	499.	13	0.0031	13	1181.0	135^{+0}_{-1}	670	0.0030	13
197.3	3400.		0.0082	15	197.3	3400.		0.0152	15	197.4 [a]		3400	0.0092	15
										197.3	136	2800	0.0060	8
381.5	3400.		0.0059	22	381.1	3400.		0.0176	20	381.6 [a]		3400	0.0086	20
										380.7	136	3400	0.0073	8
1313.9	3400.		0.0095	30	1313.4	3400.		0.0156	35	1313.4 [a]		3400	0.0086	35
										1313.3	136	3000	0.0057	24
314.3	8.2	10	0.0055	60	314.1	8.7	10	0.0082	60	314.4	138^{+0}_{-1}	9	0.0039	8
400.1	7.8	10	0.0059	80	400.1	8.1	10	0.0075	80	400.2	138^{+0}_{-1}	9	0.0037	9

[a] Data for these γ rays are from the present experiment.

in ^{136}Xe (Ref. 15). A γ ray at 1320.2 ± 1.0 keV was also observed following β decay and was placed in cascade between the 381.7- and 1313.2-keV γ rays in the suggested decay scheme (Ref. 15). A transition corresponding to the 1320.2-keV γ ray was not observed in the present experiment or in the Livermore ^{252}Cf measurement. Consequently the present results as well as the Livermore results support the level structure given in the proton inelastic scattering results (Ref. 14). The weighted average of the 3.4-μsec γ rays is 0.0075 ± 0.0009 per fission for ^{235}U and 0.0161 ± 0.0019 per fission for ^{239}Pu for the present experiment. The systematic uncertainties of ~±10% for ^{235}U and ±15% for ^{239}Pu are not included in the values. These results agree well with the previous results (Ref. 9) of 0.0063 ± 0.0020 and 0.013 ± 0.003 per fission for ^{235}U and ^{239}Pu; additional uncertainties of ±20% existed in the previous data as a result of the normalization. In part, the difference in the results may be due to the use of a fission-neutron spectrum in the previous experiment instead of thermal neutrons, so that the fission-fragment mass distributions were somewhat different from those of the present experiment. However, most of the difference is expected to result from experimental uncertainties and normalization uncertainties (Ref. 9) in the previous data.

The ~170-nsec isomer from $^{134}_{52}Te_{82}$ and 3.4-μsec isomer from $^{136}_{54}Xe_{82}$ account for a significant fraction of the high-energy γ rays emitted in the time region studied. As pointed out by John *et al.*, the striking similarity of the γ-ray cascades for the two isomers can be explained by the difference of only a proton pair in the $^{134}_{52}Te_{82}$ and $^{136}_{54}Xe_{82}$ nuclei (Ref. 4).

If the intensity of an observed γ ray is sufficiently high, and if the value of A is known for the isomer, then the value of the atomic number Z may be determined from known information on fission-fragment yields (Ref. 16). Using the present intensity measurements for delayed γ rays and using the mass number determined at Livermore (Ref. 4), the Z value for the ~170-nsec isomer was determined to be 52; this agrees with the conclusion for Z reached by John *et al.* (Ref. 4), as discussed above. The observed transition intensities for the 170-nsec isomer and the fission yields (Ref. 16) indicate that the ratio of the fission yield for this isomer to the total direct fission yield for the fragment ($^{136}_{54}Xe_{82}$) is roughly 50% for the ^{235}U and ^{239}Pu data. In the same manner as above, the 3.4-μsec isomer was determined to have a Z of 53 or 54, which is consistent with the value of 54 given above. If one assumes a mass number of $A = 95$ for 204.3- and 352.2-keV γ rays, then the Z of the isomer is determined (Ref. 16) to be 38. Similarly, the Z of the 614.2-keV γ ray is probably 40, assuming 100 (Ref. 4) for the A value.

5. CONCLUSIONS

The present delayed γ-ray results from the thermal-neutron fission of ^{235}U and ^{239}Pu essentially fill the previous gap in the ^{235}U and ^{239}Pu data for times between the prompt γ rays and γ rays emitted later than 2 μsec after fission (Ref. 9). Eighty resolved γ-ray peaks with different energies and half-lives were observed in the ^{235}U and ^{239}Pu data. Many of these correspond to γ rays which were previously observed from ^{252}Cf studies (Ref. 4); 37 of the observed peaks had not been seen in previous delayed γ-ray measurements. Many of the new peaks are expected to be from the lower hump of the mass-yield curve, since the lower hump shifts more in mass position than the upper one for the three cases of fission considered here. Also, some of the new resolved γ-ray peaks could have been observed in the present experiment because of the higher γ-ray detector efficiency, particularly at higher energies, as compared with the Livermore detector efficiency (Ref. 4). The relatively large yield per fission for some of the γ rays indicates that the corresponding isomeric states are populated in a significant fraction of the cases in which particular fission fragments are formed. The energies and half-lives of the resolved γ rays are consistent with $E1$, $M1$, or $E2$ transitions.

The total energy of the resolved γ rays that were observed, when integrated over all time, is 163 and 164 keV/fission for ^{235}U and ^{239}Pu, respectively; the corresponding ^{252}Cf value (Ref. 4) for γ rays in the same half-life region is ~82 keV per fission, or approximately half of the ^{235}U or ^{239}Pu values. Any possible systematic difference in the ^{252}Cf results and the ^{235}U or ^{239}Pu results is much smaller than the energy difference in the resolved γ rays. Since several isomers contribute a significant fraction of the total intensity, the near equality for ^{235}U and ^{239}Pu is surprising. Of the ~80-keV difference between ^{235}U and ^{252}Cf, ~50 keV is attributable to the seven possible cascades given in Table V, and of the ~80 keV ^{239}Pu-^{252}Cf difference, ~43 keV is due to these seven isomers. These isomers are located on the low mass side of both the ^{252}Cf mass distribution peaks, where the yield is appreciably higher for ^{235}U and ^{239}Pu than that for ^{252}Cf. Roughly 40% of the total energy of the resolved γ rays in the present experiment is from 1100- to 1340-keV γ rays for both ^{235}U and ^{239}Pu. Isomers in $^{134}_{52}Te_{82}$ and

$^{136}_{54}Xe_{82}$ contribute most of these high-energy γ rays. In the 140- to 1340-keV energy range and 20- to 958-nsec time interval, the energy of the continuum of unresolved γ rays is ~20 and ~24% of the total delayed γ-ray energy for ^{235}U and ^{239}Pu, respectively.

The ratio of the number of resolved γ rays plus continuum from 20 to 958 nsec and above 140 keV (from Tables II and III) to the number of prompt γ rays above 140 keV (Ref. 6) is 3.6 and 2.9% for ^{235}U and ^{239}Pu, respectively. Maienschein *et al.* (Ref. 1) previously reported that the magnitude of the integral delayed γ-ray intensity from 50 nsec to 10 μsec after ^{235}U(n,f) is 5.7% relative to the prompt γ rays; the lower energy bias for this ratio (Ref. 1) was 160 keV, and the observed delayed γ-ray rate (Ref. 1) was negligible for 1 to 10 μsec. The lower number of delayed γ rays observed in the present experiment is possibly due to the improvement in the present timing beyond the state of the art, as well as a measurement of and a correction for the time slewing, so that the time slewing of prompt γ rays had only a small effect on the total number of delayed γ rays measured in this experiment.

In addition to the ratios for number per fission, as just discussed, the ratios for energy per fission are also of interest. The ratio of total energy per fission of the observed peaks in this experiment, integrated over all times, to the energy per fission of the prompt γ rays above 0.14 MeV (Ref. 6) is 2.5 and 2.4% for ^{235}U and ^{239}Pu, respectively. The ratio of energy per fission of the observed γ-ray peaks from 20 to 958 nsec and above 140 keV to the energy per fission of the prompt γ rays above 0.14 MeV (Ref. 6) is 1.5 and 1.3% for ^{235}U and ^{239}Pu, respectively; the observed continuum of unresolved delayed γ rays in these same regions contributes an additional ~0.4% to each of these two values.

---

*Work supported by Defense Nuclear Agency under Contract No. DASA 01-69-C-0059.

†Now at General Atomic Company, San Diego, California.

[1]F. C. Maienschein, R. W. Peele, W. Zobel, and T. A. Love, in *Proceedings of the Second United Nations International Conference on Peaceful Uses of Atomic Energy* (United Nations, Geneva, Switzerland, 1958), Vol. 15, p. 366.

[2]L. A. Popeko, G. V. Val'skii, D. M. Kaminker, and G. A. Petrov, At. Energ. 19, 186 (1965) [transl.: J. Nucl. Energy A/B 20, 811 (1966)].

[3]S. A. E. Johansson, Nucl. Phys. 64, 147 (1965).

[4]W. John, F. W. Guy, and J. J. Wesolowski, Phys. Rev. C 2, 1451 (1970).

[5]N. N. Ajitanand, Nucl. Phys. A164, 300 (1971).

[6]V. V. Verbinski, H. Weber, and R. E. Sund, Phys. Rev. C 7, 1173 (1973).

[7]R. B. Walton, R. E. Sund, E. Haddad, J. C. Young, and C. W. Cook, Phys. Rev. 134, B824 (1964).

[8]R. E. Sund and R. B. Walton, Phys. Rev. 146, 824 (1966).

[9]R. B. Walton and R. E. Sund, Phys. Rev. 178, 1894 (1969).

[10]J. T. Routti and S. G. Prussin, Lawrence Radiation Laboratory Report No. UCRL-17672, December 1, 1968 (unpublished).

[11]W. R. Burrus and V. V. Verbinski, Nucl. Instrum. Methods 67, 181 (1969).

[12]F. W. Guy, Lawrence Radiation Laboratory Report No. UCRL-50810, February 1970.

[13]L. S. Kisslinger and R. A. Sorensen, K. Dan. Vidensk. Selsk., Mat.-Fys. Medd. 32, No. 9 (1960).

[14]P. A. Moore, P. J. Riley, C. M. Jones, M. D. Mancusi, and J. L. Foster, Jr., Phys. Rev. C 1, 1100 (1970).

[15]A. Lundan and A. Süvola, Ann. Acad. Sci. Fennicae A6, No. 288 (1968).

[16]M. E. Meek and B. F. Rider, Vallecitos Nuclear Center Report No. NEDO-12154, 71 NED 41, January 1972 (unpublished).